

A NOVEL STEP UP MISO CONVERTER FOR HYBRID ELECTRICAL VEHICLES APPLICATION

Thirukumar.P¹, Akash.D¹, Sasidharan.R¹, Kamalkumar.T²

¹Under graduate Student, ²Assistant professor, Dept. of Electrical and Electronics Engineering, T.J.S Engineering College, Peruvoyal, Tamil Nadu, India

ABSTRACT

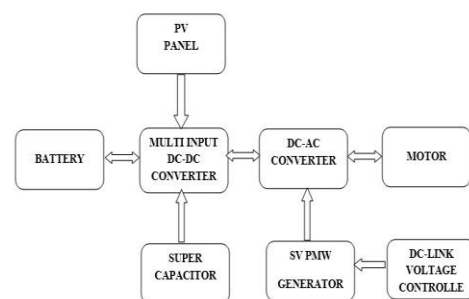
In this Project, a multi-input DC-DC converter is proposed and studied for hybrid electric vehicles (HEVs). Compared to conventional works, the output gain is enhanced, photovoltaic (PV) panel and energy storage system (ESS) are the input sources for proposed converter. The Super capacitor is considered as the main power supply and roof-top PV is employed to charge the battery, increase the efficiency and reduce fuel economy. The converter has the capability of providing the demanded power by load in absence of one or two resources. Moreover, power management strategy is described and applied in control method. A prototype of the converter is also implemented and tested to verify the analysis.

INTRODUCTION

Global warming and lack of fossil fuels are the main drawbacks of vehicles powered by oil or diesel. In order to overcome the aforementioned problems and regarding the potential of clean energies in producing electricity, car designers have shown interest in hybrid electric vehicles (HEVs) and plug-in hybrid electric vehicles (PHEVs). The overall structure of hybrid electric vehicle powered by renewable resources is depicted in Fig.1. Electric vehicles (EVs) have also been studied. EVs rely on energy stored in energy storage system (ESS). Limited driving range and long battery charging time are their main drawbacks. However, by using a bidirectional on/off board charger, they could have the V2G capability. Solar-assisted EVs have also

been studied. Required location and size of PV panels have made them impractical at present. Employing fuel cell as the main power source of HEVs is the result of many years of research and development on HEVs. Pure water and heat are the only emissions of fuel cells. Furthermore, SUPER CAPACITORS have other advantages like high density output current ability, clean electricity generation, and high efficiency operation. However, high cost and poor transient performance are the main problems of SUPER CAPACITORS. It is important to note that vehicles mainly powered by SUPER CAPACITORS, are hybridized by ESSs. The main advantages of hybridizing are enhancing fuel economy, providing a more flexible operating strategy, overcoming fuel cell coldstart and transient problems and reducing the cost per unit power.

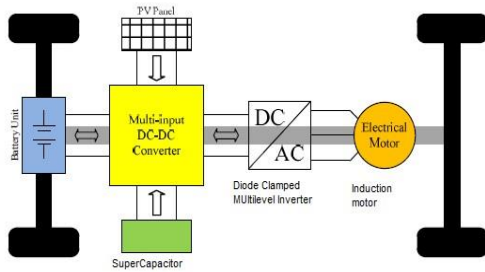
BLOCK DIAGRAM OF PROPOSED SYSTEM



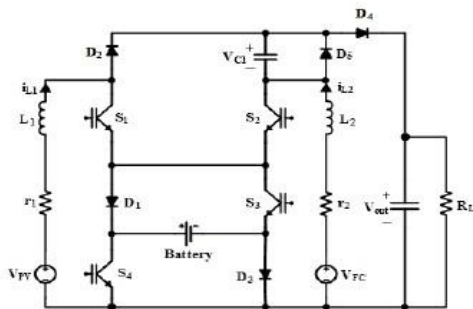
Due to the fact that initial cost of PVs is high and in order to increase the extracted power from the PV panels, MPPT algorithm has to be utilized. A general comparison is made between different MPPT techniques

with respect to tracking factor, dynamic response, PV voltage ripple and use of sensors. The other way to improve the efficiency is to enhance the efficiency of the electric components

GENERAL STRUCTURE OF MULTI-POWERED HEV Modules Description: Circuit Diagram



General Structure of Multi-Powered HEV



Three-Input DC-DC Boost Converter

Operation of the converter is divided into three states: 1- The load is supplied by PV and SUPER CAPACITOR and battery is not used. 2- The load is supplied by PV, SUPER CAPACITOR and battery, in this state battery is in discharging mode. 3- The load is supplied by PV and SUPER CAPACITOR and battery is in charging mode.

Operation Modes

First operation state (The load is supplied by PV and SC while battery is not used):

In this state, as it is illustrated in Fig. 3, there are three operation modes.

During this state, the system is operating without battery charging or discharging.

Therefore, there are two paths for current to flow (through S3 and D3 or D1 and S4). In this paper S3 and D3 is considered as common path. However, D1 and S4 could be chosen as an alternative path. During this state, switch S3 is permanently ON and switch S4 is OFF.

Mode 1 (0 < t < d1T): In this interval, switches S1, S2, S3 and diode D3 are turned ON. Inductors L1 and L2 are charged via power sources v_{PV} and v_{SUPER CAPACITOR}, respectively [see Fig. 3(a)].

$$L_1: d_1[V_{PV} - r_1 i_{L1}] + (d_2 - d_1)[V_{PV} - r_1 i_{L1} - V_{C1}] + (1 - d_2)[V_{PV} - r_1 i_{L1}] = 0 \tag{1}$$

$$V_{C1} = \frac{V_{PV} - r_1 i_{L1}}{d_2 - d_1} \tag{2}$$

$$L_2: d_2[V_{FC} - r_2 i_{L2}] + (1 - d_2)[V_{FC} + V_{C1} - r_2 i_{L2} - V_o] = 0 \tag{3}$$

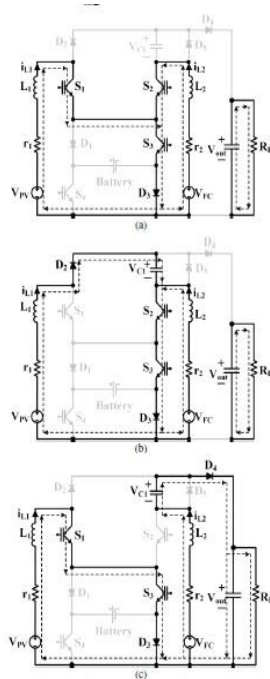
$$V_o = \frac{(d_2 - d_1)(V_{FC} - r_2 i_{L2}) + (1 - d_2)(V_{FC} - r_1 i_{L1})}{(1 - d_2)(d_2 - d_1)} \tag{4}$$

Mode 2 (d1T < t < d2T): In this interval, switch S1 is turned OFF and D2 is turned ON and S2, S3 and D3 are still ON. Inductor L2 is still charged and inductor L1 is being discharged via v_{PV}-v_{C1}[see Fig. 3(b)].

Mode 3 (d2T < t < T): In this interval, S1 is turned ON and S2 is turned OFF and S3 and D3 are still ON. Inductor L1 is charged with v_{PV} and inductor L2 is discharged via v_{PV}+v_{C1} - v_o[see Fig. 3(c)]. By applying the

voltage–second balance low over the inductors L1 and L2, voltage of capacitor C1 and output voltage can be obtained as follows: Also, by applying the current–second balance low over the capacitors C1 and Co, voltage of capacitor C1, we have

$$C_1 : (d_2 - d_1)i_{L_1} - (1 - d_2)i_{L_2} = 0 \tag{5}$$



Current-Flow Path of Operating Modes In First Operating State. (A) Mode 1.(B) Mode 2. (C) Mode.

Second operation state (The load is supplied by PV, SUPER CAPACITOR and battery)

In this state, as it is illustrated in Fig. 4, there are four operation modes.

During this state, the load is supplied by all input sources (PV, SUPER CAPACITOR and battery). In first mode there is only one current path. However, in other three modes, there are two current paths (through S3 and D3 or D1 and S4). In this state, current flows through D1 and S4. Switch S4 is permanently ON during this state.

Mode 1 (0 < t < d1T): In this interval, S1, S2, S3 and S4 are turned ON. Inductors L1 and L2

are charged by vPV + vBattery and vSUPER CAPACITOR + vBattery respectively[see Fig. 4(a)].

Mode 2 (d1T < t < d2T): In this interval, S1, S2, S4 and D1 are turned ON. Inductors L1 and L2 are charged by vPV and vSUPER CAPACITOR respectively

Mode 3 (d2 T < t < d3T): In this interval, S2, S4, D1 and D2 are turned ON. Inductor L1 is discharged to capacitor C1 and L2 is charged by vSUPER CAPACITOR.

Mode 4 (d3T < t < d4T): In this interval, S1, S4, D1 and D4 are turned ON. Inductor L1 is charged by vPV and inductor L2 discharges C1 to the output capacitor. [see Fig. 4(d)]. By applying the voltage–second balance low over the inductors L1 and L2, we have:

$$L_1 : d_1 [V_{PV} + V_{bat} - r_1 i_{L_1}] + (d_2 - d_1) [V_{PV} - r_1 i_{L_1}] + (d_3 - d_2) [V_{PV} - r_1 i_{L_1} - V_{C_1}] + (1 - d_3) [V_{PV} - r_1 i_{L_1}] = 0 \tag{8}$$

And then:

$$V_{C_1} = \frac{V_{PV} + d_1 V_{bat} - r_1 i_{L_1}}{d_3 - d_2} \tag{9}$$

$$L_2 : d_1 [V_{RC} + V_{bat} - r_2 i_{L_2}] + (d_3 - d_1) [V_{RC} - r_2 i_{L_2}] + (1 - d_3) [V_{RC} + V_{C_1} - r_2 i_{L_2} - V_o] = 0 \tag{10}$$

And then:

$$V_o = \frac{(d_3 - d_2)(V_{RC} + d_1 V_{bat} - r_2 i_{L_2}) + (1 - d_3)(V_{PV} + d_1 V_{bat} - r_1 i_{L_1})}{(1 - d_3)(d_3 - d_2)}$$

Also, by applying the current–second balance low over the capacitors C1 and Co, voltage of capacitor C1, we have:

$$C_1 : (d_3 - d_2)i_{L_1} - (1 - d_3)i_{L_2} = 0 \tag{12}$$

$$C_o : (1 - d_3)i_{L_2} = \frac{V_o}{R_{Load}} \tag{13}$$

In this state, the current and power of battery can be calculated as (14) and (15) respectively:

$$i_{bat} = d_1 (i_{L_2} + i_{L_1}) \quad (14)$$

$$P_{bat} = V_{bat} [d_1 (i_{L_2} + i_{L_1})] \quad (15)$$

Third operation state (The load is supplied by PV and SUPERCAPACITOR while battery is in charging mode)

In this state, as it is illustrated in Fig. 5, there are four modes. During this state, PV and SUPER CAPACITOR charges the battery and supply the energy of load. In the first and second operation modes, there are two possible current paths through S3 and D3 or D1 and S4). The path D1 and S4 is chosen to flow the current in this state. During this state, switch S3 is permanently OFF and diode D1 conducts.

Mode 1 (0 < t < d1T): In this interval, S1, S2, S4 and D1 are turned ON. Inductors

L1 and L2 are charged by vPV and vSUPER CAPACITOR, respectively [see Fig. 5(a)].

Mode 2 (d1T < t < d2T): In this interval, S2, S4 and D1 are turned ON. Inductor L1 is discharged to capacitor C1 and,

Mode 3 (d2 T < t < d3 T): In this interval, S1, S2, D1 and D3 are turned ON. Inductors L1 and L2 are charged by vPV – vBattery and vSUPER CAPACITOR – vBattery, respectively [see Fig. 5(c)].

Mode 4 (d3 T < t < d4 T): In this interval, S1, S4, D1 and D4 are turned ON. Inductor L1 is charged by vPV - vBattery and inductor L2 is discharged by vSUPER CAPACITOR– vC1 – v0

By applying the voltage–second balance law over the inductors L1 and L2, we have:

$$L_1: d_1 [V_{PV} - r_1 i_{L_1}] + (d_2 - d_1) [V_{PV} - r_1 i_{L_1} - V_{C_1}] + (1 - d_2) [V_{PV} - r_1 i_{L_1} - V_{bat}] = 0 \quad (16)$$

$$V_{C_1} = \frac{V_{PV} - (1 - d_2) V_{bat} - r_1 i_{L_1}}{d_2 - d_1} \quad (17)$$

$$L_2: d_2 [V_{FC} - r_2 i_{L_2}] + (d_3 - d_2) [V_{FC} - r_2 i_{L_2} - V_{bat}] + (1 - d_3) [V_{FC} + V_{C_1} - r_2 i_{L_2} - V_o] = 0 \quad (18)$$

$$V_o = \frac{(V_{FC} - (d_3 - d_2) V_{bat} - r_2 i_{L_2})}{(1 - d_3)} \quad (19)$$

$$+ \frac{(V_{PV} - (1 - d_2) V_{bat} - r_1 i_{L_1})}{(d_2 - d_1)}$$

By applying current-second balance law to capacitors C1 and Co, we have:

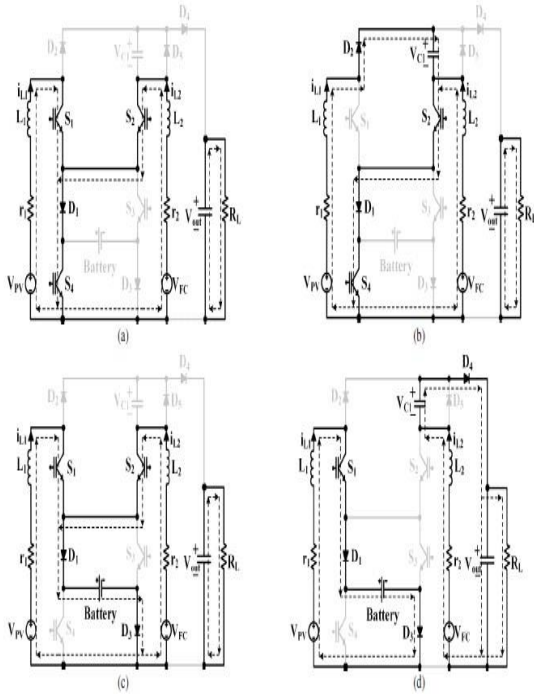
$$C_1: (d_2 - d_1) i_{L_1} - (1 - d_3) i_{L_2} = 0$$

In this state, the current and delivered power by battery can be obtained as (22) and (23):

$$i_{bat} = (d_3 - d_2) (i_{L_2} + i_{L_1}) + (1 - d_3) i_{L_1} \quad (22)$$

$$P_{bat} = V_{bat} [(d_3 - d_2) (i_{L_2} + i_{L_1}) + (1 - d_3) i_{L_1}] \quad (23)$$

Illustrates switching pattern for each state and each mode. To fulfill switching operation, a saw-tooth wave as a carrier is compared with signals d1, d2, d3 and d4, which can independently control on state of power switches. Without considering output voltage utilized power of each sources PV, SUPER CAPACITOR and battery can be controlled using d1, d2, d3 and d4 signals. [24]



Current-Flow Path of Operating Modes In Third Operating State.

(a) Mode 1. (b) Mode 2. (c) Mode 3. (d) Mode 4.

As shown in this figure, the voltage gain of the proposed converter is higher than the converter proposed in [24]. Benefiting from high voltage gain, the proposed converter achieve the specific output voltage V_O with less duty cycles in comparison with the converter proposed in [24]

which increase the efficiency of the proposed converter. It is worth noting that in this figure, the inductor resistances are ignored and the voltage gain is compared in the first operation mode. Input voltages are also considered the same.

Output Voltage Waveform

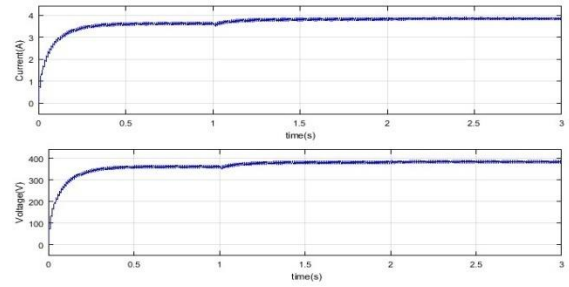
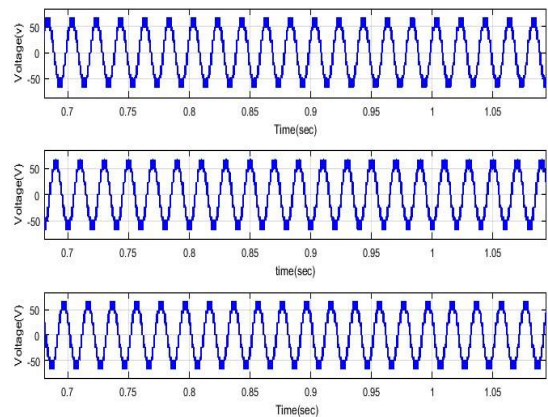


Fig.4.16. Output Wave Form

Battery Waveform

Battery Waveform



. Low-Cost Target Hardware

CONCLUSION

The suggested converter Topology consists of three level hybrid boost dc-dc converter and Three phase 5-level DCMLI, In hybrid boost dc-dc converter, stepup the fuel cell output voltage with high voltage gain. It is not only improving the converter's performance but also controls the duty ratio to minimum value. Here, boost inductor, ripple current and voltage are derived with respect to converter parameters. The dynamic and steady state performance of both the capacitors are verified and voltages across the filtering capacitors are balanced by the PWM control technique. The major advantage with this converter, the voltage across the power

switches is half of the output voltage. The output of DC voltage is again converted in to AC by using multilevel inverter. This converter topology is better for fuel cell based electric vehicle.

. In the future we can use some other converter with this super capacitor that may increase the efficiency and output of the system.

REFERENCES

[1] A. Ostadi, and M. Kazerani. "Optimal Sizing of the Battery Unit in a Plug-in

Electric Vehicle," Vehicular Technology, IEEE Transactions on, vol.63, no.7, pp.3077-3084, Sept. 2014.

[2] P. Mulhall , S. M. Lukic , S. G. Wirashingha , Y.-J. Lee and A.

Emadi "Solarassisted electric auto rickshaw three wheeler", Vehicular Technology,

IEEE Transactions on, vol. 59, no. 5, pp.2298 - 2307 2010.

[3] H. J. Chiu, and L. W. Lin. "A bidirectional DC-DC converter for fuel cell electric vehicle driving system", IEEE Trans. Power Electron., vol. 21, no. 4, pp.950 -958, 2006.

[4] T. Markel, M. Zolot, K. B. Wipke, and A. A. Pesaran. "Energy storage requirements for hybrid fuel cell vehicles", 2003, Advanced Automotive Battery Conf.

[5] S. Miaosen. "Z-source inverter design, analysis, and its application in fuel cell vehicles", Ph.D. dissertation, Michigan State Univ., East Lansing, USA, 2007.

[6] O. Hegazy, R. Barrero, J. Van Mierlo, P. Lataire, N. Omar and T. Coosemans. "An Advanced Power Electronics Interface for Electric Vehicles Applications," IEEE Trans. Power Electron, Vol. 28, No. 12, pp. 1-14, Dec. 2013.